Dalton Transactions

Accepted Manuscript

This article can be cited before page numbers have been issued, to do this please use: D. P. Malenov and S. D. Zaric, *Dalton Trans.*, 2019, DOI: 10.1039/C9DT00182D.

ROYAL SOCIETY OF CHEMISTRY

rsc.li/dalton

ROYAL SOCIETY OF CHEMISTRY
View Article Online
DOI: 10.1039/C9DT00182D

Dalton Transactions

COMMUNICATION

Strong stacking interactions of metal-chelate rings are caused by substantial electrostatic component

Dušan P. Malenov[a,b] and Snežana D. Zarić*[,a,b]

Z Received 00th January 20xx,
Accepted 00th January 20xx

DOI: 10.1039/x0xx00000x

www.rsc.org/

Symmetry Adapted Perturbation Theory (SAPT) analysis shows that stacking interactions of metal-chelate rings are stronger than stacking interactions of organic molecules due to much stronger electrostatic interactions caused by the presence of metal. Depending on the ligand, electrostatic component of chelate stacking can be stronger than dispersion component.

Stacking interactions of aromatic fragments are of great importance for many chemical and biological systems.[1–3] They are among the crucial factors for stability of structures of nucleic acids[4,5] and play an important role in the structure of proteins.[6,7] Important systems that can form various noncovalent interactions are metal-chelate rings,[8–11] which are widespread in materials science,[12] catalysis[13–15] and crystal engineering.[8] Metal-chelate rings with delocalized π-bonds were considered to be aromatic,[16] but it was later determined that many of them do not satisfy magnetic criteria of aromaticity.[17] Nevertheless, chelate rings frequently form stacking interactions with both aromatic[18–21] and other chelate rings,[22–26] as evidenced by the analysis of crystal structures from the CSD.[8] Moreover, there are many studies showcasing that stacking interactions between nonaromatic moieties are stronger than those of aromatic moieties.[8,27–29]

Our previous DFT-D calculations revealed that stacking interactions of chelate rings are stronger than stacking interactions between organic aromatic rings. Benzene-chelate stacking interactions of *acac*-type Ni chelate (-5.49 kcal/mol)[30] and of dithiolene Ni chelate (-5.43 kcal/mol)[31] are significantly stronger than the stacking between two benzene molecules (-2.73 kcal/mol),[28] or between benzene and pyridine (-3.54 kcal/mol).[32] Chelate-chelate stacking is even stronger; stacking energy between two *acac*-type Ni chelates is -9.50 kcal/mol,[33] and between two Ni dithiolene chelates -10.34 kcal/mol.[31] Previous results have also shown that interaction energies can be different depending on a particular metal and ligand.[8,31,33] The calculations showed that the strongest benzene-chelate stacking interactions have parallel-displaced geometries,[30] which is in agreement with the dominance of these geometries in crystal structures.[8] The strongest chelate-chelate stacking interactions can also have geometries very similar to sandwich,[33] which is also in agreement with the data found in crystal structures.[8]

In this work we study the nature of metal-chelate stacking interactions by performing the energy decomposition analysis of benzene-chelate (**Bz-Ch**) and chelate-chelate (**Ch-Ch**) stacking based on Symmetry Adapted Perturbation Theory (SAPT)[34]. The results on stacking interactions of chelate rings were compared with SAPT analysis of stacking interactions of organic molecules.[35,36] To the best of our knowledge, these are the first results of energy decomposition SAPT analysis of stacking interactions of chelate rings.

In order to study the influence of metals on stacking interactions of chelate rings, we have used Ni, Cu and Zn complexes that contain six-membered chelate ring of *acac* type (Figure 1). The influence of ligand was studied by comparing the results for nickel *acac*-type chelate rings, which contain oxygen, with the results for nickel dithiolene chelate rings, which contain sulfur (Figure 2).

Figure 1. Minimum geometries of benzene-chelate (**Bz-Ch**) and chelate-chelate (**Ch-Ch**) stacking interactions of ***acac***-type chelate rings of Ni, Cu and Zn. The corresponding potential energy curves are presented in ESI (Figures S4 and S6).

Benzene-chelate and chelate-chelate stacking geometries were described by two geometrical parameters – horizontal displacement (offset) **r** and normal distance **R** (Figure 3). By

[a] *Faculty of Chemistry, University of Belgrade, Studentski trg 12-16, 11000 Belgrade, Serbia. E-mail: szaric@chem.bg.ac.rs.*
[b] *Department of Chemistry, Texas A&M University at Qatar, P.O. Box 23874, Doha, Qatar.*

Electronic Supplementary Information (ESI) available: potential energy curves for benzene-chelate and chelate-chelate stacking, additional SAPT analysis data. See DOI: 10.1039/x0xx00000x

View Article Online DOI: 10.1039/C9DT00180D

changing the normal distances for a series of offset values, we have calculated the potential energy curves for stacking interactions of chelate rings (ESI), and performed the SAPT analysis of the curve minima (Figures 1 and 2).

Figure 2. Minimum geometries of benzene-chelate (**Bz-Ch**) and chelate-chelate (**Ch-Ch**) stacking interactions of **dithiolene** chelate rings of Ni. The corresponding potential energy curves are presented in ESI (Figures S4 and S6).

In our previous works we reported benzene-chelate stacking energies for Ni and Cu chelates,[30,31] as well as the chelate-chelate stacking energies between two Ni chelates.[33] In this work, we additionally calculated benzene-chelate and chelate-chelate stacking energies for Zn complex, as well as chelate-chelate stacking energies for Cu complex. Zn chelates form the strongest stacking interactions, with the strongest benzene-chelate energy of -7.56 kcal/mol (**Bz-Ch min2** geometry, Figure 1), and the strongest chelate-chelate energy of -14.58 kcal/mol (**Ch-Ch min** geometry, Figure 1).

The PSI4 program package[37] was used for all SAPT calculations. For the Ni and Zn chelates, all SAPT levels can be applied (ESI). However, only SAPT0[38–40] is applicable for open-shell systems, as is our *acac*-type Cu complex, and it was therefore used in this work. The calculated total SAPT0 energies are in reasonable agreement with DFT-D energies (Tables 1 and 2), which were used to obtain potential energy curves (ESI).

To study the influence of metals on stacking of metal-chelate rings, the SAPT0 analysis of stacking of *acac*-type chelates of Ni, Cu and Zn was performed for the minima at potential energy curves (Figure 1). For benzene-chelate stacking (**Bz-Ch**) the results show that for all three metals and for both minimum geometries the strongest stabilizing component is dispersion. However, the largest part of dispersion is cancelled by the exchange term, leading to net dispersion that is of low magnitude in comparison to overall interaction energy (Table 1). Considering that, SAPT0 analysis implies that the strong electrostatic component is responsible for the strong benzene-chelate stacking.

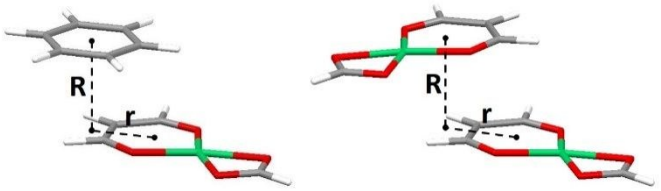

Figure 3. The geometrical parameters describing the benzene-chelate and chelate-chelate stacking interactions are the horizontal displacement (offset) r of the centers of interacting rings, and the normal distance R, presented here as the shortest distance between benzene ring center and the chelate plane (**Bz-Ch**) or between center of one chelate ring and the plane of the other chelate ring (**Ch-Ch**)

For chelate-chelate stacking of *acac*-type rings, SAPT0 analysis showed that for all three metals electrostatic component is significantly more favorable than it is for benzene-chelate stacking; it is even stronger than dispersion for all the geometries (Table 1). Moreover, net dispersion can be very unfavourable (Table 1), which makes electrostatic component even more important for chelate-chelate stacking than for benzene-chelate stacking.

Table 1. Geometrical parameters (offset **r** and normal distance **R**) and interaction energies (in kcal/mol) calculated at DFT-D and SAPT0 levels for minima at potential energy curves (**Bz-Ch min1**, **Bz-Ch min2**, and **Ch-Ch min**, Figure 1) of ***acac***-type benzene-chelate and chelate-chelate stacking. The SAPT0 energies consist of electrostatic (ELST), dispersion (DISP), exchange (EXCH) and induction component (IND). The sum of dispersion and exchange components is usually regarded as net dispersion (DISP + EXCH = NET DISP).[35,41]

***acac* Bz-Ch min1**	**r [Å]**	**R [Å]**	**ωB97X-D/ def2-TZVP [a]**	**SAPT0/ def2-TZVP**	**ELST**	**DISP**	**EXCH**	**IND**	**NET DISP**
Ni	1.3	3.40	-4.82	-5.12	-3.63	-8.06	+7.40	-0.82	-0.66
Cu	1.2	3.40	-4.92	-5.24	-3.81	-8.21	+7.63	-0.87	-0.58
Zn	1.0	3.43	-4.93	-5.18	-3.72	-8.09	+7.48	-0.85	-0.61
***acac* Bz-Ch min2**	**r [Å]**	**R [Å]**	**ωB97X-D/ def2-TZVP [a]**	**SAPT0/ def2-TZVP**	**ELST**	**DISP**	**EXCH**	**IND**	**NET DISP**
Ni	1.4	3.37	-5.52	-5.97	-4.07	-9.00	+7.91	-0.80	-1.09
Cu	1.3	3.31	-6.43	-6.80	-5.38	-9.78	+9.53	-1.16	-0.25
Zn	1.3	3.27	-7.56	-7.59	-6.38	-10.12	+10.52	-1.61	+0.40
***acac* Ch-Ch min**	**r [Å]**	**R [Å]**	**LC-ωPBE-D3BJ/ aug-cc-pVDZ [b]**	**SAPT0/ def2-TZVP**	**ELST**	**DISP**	**EXCH**	**IND**	**NET DISP**
Ni	0.5	3.13	-9.47	-10.11	-11.99	-11.89	+15.60	-1.82	+3.71
Cu	0.4	3.01	-11.70	-12.54	-16.67	-13.82	+21.42	-3.47	+7.60
Zn	0.4	2.88	-14.58	-15.39	-23.21	-16.18	+30.67	-6.67	+14.49

[a] ωB97X-D is in good agreement with CCSD(T)/CBS for benzene-chelate stacking;[30] [b] LC-ωPBE-D3BJ/aug-cc-pVDZ is in good agreement with CCSD(T)/CBS for chelate-chelate stacking[33]

Electrostatic potential maps (Figure 4) can help in understanding the stacking interactions of metal-chelate rings. Strong *acac*-type benzene-chelate stacking interactions in the most stable geometry (**Bz-Ch min2**, Figure 1) are the consequence of overlapping of negative electrostatic potential above benzene and positive potential above the metal of the

chelate ring (Figure 4). *Acac*-type chelate-chelate stacking in the most stable geometry (**Ch-Ch min**, Figure 1) is even stronger, since there is the overlap of negative potential above C2 ring of one chelate and positive potential above metal of the other chelate, and vice versa (Figure 4). For both benzene-chelate and chelate-chelate stacking, the strong electrostatic component increases from Ni to Zn, since the magnitudes of positive electrostatic potentials increase from Ni to Zn (Figure 4). For that reason, zinc chelate forms the strongest benzene-chelate and chelate-chelate stacking interactions in the most stable geometries. The same trends (Table S1, ESI) are present in sandwich geometries for both benzene-chelate and chelate-chelate stacking (Figure S3, ESI). However, in **Bz-Ch min1** geometry of benzene-chelate stacking, the metal influence is not large (Figure 1), hence the overall stacking energies and all their components are very similar for all metals (Table 1).

As was mentioned above, to study the influence of ligands on stacking interactions, we have compared the stacking energies of *acac*-type (Figure 1) and dithiolene chelates of Ni (Figure 2). For these calculations we have used the neutral nickel *bis*(dithiolene) complex.[42] The data in Tables 1 and 2 do not show large differences in interaction energies for Ni complexes with these two types of ligands, while the components of the interaction energies are quite different, indicating different nature of the interactions.

Due to the presence of voluminous sulfur atoms, normal distances are higher for dithiolene stacking (Table 2) than for *acac*-type stacking (Table 1). Presence of sulfur also causes dispersion to be the strongest energy component for all the geometries for both benzene-chelate and chelate-chelate stacking of Ni dithiolene (Table 2). However, net dispersion is of low magnitude (Table 2), meaning that electrostatic component is the most responsible for strong stacking of dithiolene chelates. We want to point out that SAPT0 overestimates dithiolene benzene-chelate stacking (Table 2), particularly in the most stable **Bz-Ch min2** geometry (Figure 2). More consistent SAPT2 data (Tables S3 and S5, ESI) show that electrostatic component is less pronounced for dithiolene than for *acac*-type chelates, which is in agreement with their electrostatic potentials (Figure 4). However, the strongest benzene-chelate stacking interactions (**Bz-Ch min2**) of dithiolene and *acac*-type chelates are of similar energies, since induction term is more pronounced for dithiolene stacking (Table 2).

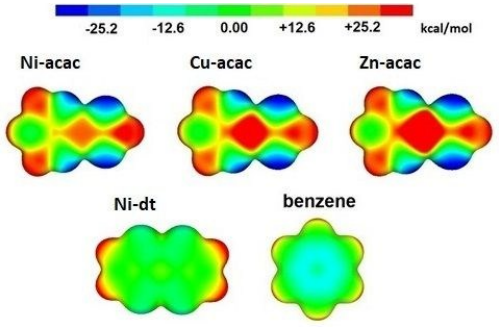

Figure 4. Electrostatic potentials plotted at the surface defined by the electron density of 0.004 a.u. for benzene molecule and chelates of nickel, copper and zinc.

For chelate-chelate stacking electrostatic component is significantly less strong for dithiolene than for *acac*-type chelate (Tables 1 and 2). However, for dithiolene chelates, electrostatic component is still much more dominant than net dispersion (Table 2), which means that electrostatic component is the reason for strong dithiolene chelate-chelate stacking. In spite of weaker electrostatic component in chelate-chelate stacking for dithiolene than for *acac*-type chelate (Tables 1 and 2), dithiolene stacking is somewhat stronger than *acac*-type, since dithiolene stacking has stronger net dispersion and stronger induction component (Tables 1 and 2). It should also be noted that net dispersion is favourable for Ni chelate-chelate dithiolene stacking (Table 2), while it is unfavourable for Ni *acac*-type chelate-chelate stacking (Table 1).

Table 2. Geometrical parameters (offset **r** and normal distance **R**) and interaction energies (in kcal/mol) calculated at DFT-D and SAPT0 levels for benzene-chelate (Bz-Ch) and chelate-chelate (Ch-Ch) stacking of Ni dithiolene (***dt***) chelate.

Ni *dt*	r [Å]	R [Å]	DFT-D [a]	SAPT0/ cc-pVDZ	ELST	DISP	EXCH	IND	NET DISP
Bz-Ch min1	1.5	3.50	-4.78	-4.99	-3.73	-7.98	+7.94	-1.22	-0.04
Bz-Ch min2	1.8	3.61	-5.43	-6.60	-4.60	-11.62	+11.14	-1.52	-0.48
Ch-Ch min	1.8	3.61	-10.14	-13.28	-8.37	-21.24	+19.79	-3.46	-1.45

[a] ωB97X-D/6-31+G* was used for benzene-chelate and PBE0-D3BJ/6-31G* for chelate-chelate stacking, since they are in good agreement with CCSD(T)/CBS energies[31]

SAPT analysis can indicate the differences in nature of stacking interactions of chelate rings and organic aromatic molecules. SAPT analysis showed that dispersion is the most dominant component for stacking of organic aromatic molecules, but it is mostly cancelled by exchange component, resulting in very small net dispersion.[35] Net dispersion is also very small for benzene-chelate stacking interactions (Tables 1 and 2), while it can be strongly destabilizing for chelate-chelate stacking (Table 2). Therefore, electrostatic component is the most important stabilizing force for organic aromatic stacking,[35,36] for benzene-chelate stacking (Tables 1 and 2), and particularly for chelate-chelate stacking (Table 1). However, electrostatic interactions of chelate rings can be much stronger than those of aromatic rings, and therefore stacking of chelate rings is much stronger than stacking of organic rings. Additional stabilization of chelate stacking can be provided by induction component (Tables 1 and 2), which is not particularly pronounced for organic stacking.[35]

In a conclusion, SAPT analysis shows that electrostatic component is the most responsible for the strength of stacking interactions of metal-chelate rings. Metal atoms in chelate rings influence the stacking significantly; for *acac*-type chelates electrostatic component increases from Ni to Zn chelates.

Chelate-chelate stacking is stronger than benzene-chelate stacking, and the stacking energies for both interaction types increase from Ni to Zn chelates. Presence of sulfur atom in Ni dithiolene chelate causes increase of the dispersion component in comparison to *acac*-type chelate. Stacking interactions of chelate rings are stronger than stacking interactions of organic aromatic rings due to stronger electrostatic energy component.

Acknowledgements

This work was supported by the Ministry of Science, Education and Technological Development of the Republic of Serbia (grant 172065). The HPC resources and services used in this work were provided by the IT Research Computing group in Texas A&M University at Qatar, which is funded by the Qatar Foundation for Education, Science and Community Development (http://www.qf.org.qa).

Conflicts of interest

There are no conflicts to declare.

Notes and references

1 L. M. Salonen, M. Ellermann and F. Diederich, *Angew. Chemie - Int. Ed.*, 2011, **50**, 4808–4842.
2 C. Janiak, *Dalton Trans.*, 2000, **95**, 3885–3896.
3 E. Ahmed, D. P. Karothu and P. Naumov, *Angew. Chemie Int. Ed.*, 2018, **57**, 8837–8846.
4 V. L. Malinovskii, F. Samain and R. Häner, *Angew. Chemie Int. Ed.*, 2007, **46**, 4464–4467.
5 C. A. Hunter and J. K. M. Sanders, *J. Am. Chem. Soc.*, 1990, **112**, 5525–5534.
6 Q. Hou, R. Bourgeas, F. Pucci and M. Rooman, *Sci. Rep.*, 2018, **8**, 14661.
7 S. Balakrishnan and S. P. Sarma, *Biochemistry*, 2017, **56**, 4346–4359.
8 D. P. Malenov, G. V. Janjić, V. B. Medaković, M. B. Hall and S. D. Zarić, *Coord. Chem. Rev.*, 2017, **345**, 318–341.
9 E. R. T. Tiekink and J. Zukerman-Schpector, *Chem. Commun.*, 2011, **47**, 6623.
10 E. R. T. Tiekink, *Coord. Chem. Rev.*, 2017, **345**, 209–228.
11 P. Cassoux, L. Valade, H. Kobayashi, A. Kobayashi, R. A. Clark and A. E. Underhill, *Coord. Chem. Rev.*, 1991, **110**, 115–160.
12 E. Coronado and P. Day, *Chem. Rev.*, 2004, **104**, 5419–5448.
13 H. Jacobsen and J. P. Donahue, *Inorg. Chem.*, 2008, **47**, 10037–10045.
14 Y. Fan and M. B. Hall, *J. Am. Chem. Soc.*, 2002, **124**, 12076–12077.
15 L. Dang, M. F. Shibl, X. Yang, D. J. Harrison, A. Alak, A. J. Lough, U. Fekl, E. N. Brothers and M. B. Hall, *Inorg. Chem.*, 2013, **52**, 3711–3723.
16 H. Masui, *Coord. Chem. Rev.*, 2001, 219–221, 957–992.
17 M. K. Milčić, B. D. Ostojić and S. D. Zarić, *Inorg. Chem.*, 2007, **46**, 7109–7114.
18 H. H. Monfared, M. Vahedpour, M. M. Yeganeh, M. Ghorbanloo, P. Mayer and C. Janiak, *Dalt. Trans.*, 2011, **40**, 1286–1294.
19 T. S. Basu Baul, S. Kundu, S. Mitra, H. Höpfl, E. R. T. Tiekink and A. Linden, *Dalton Trans.*, 2013, **42**, 1905–20.
20 T. S. Basu Baul, S. Kundu, H. Höpfl, E. R. T. Tiekink and A. Linden, *J. Coord. Chem.*, 2014, **67**, 1061–1078.
21 A. Sousa-pedrares, J. A. Viqueira, J. Antelo, E. Labisbal, J. Romero, A. Sousa, O. R. Nascimento and J. A. García-vázquez, *Eur. J. Inorg. Chem.*, 2011, **2011**, 2273–2287.
22 K. F. Konidaris, A. K. Powell and G. E. Kostakis, *CrystEngComm*, 2011, **13**, 5872.
23 L. Holland, W.-Z. Shen, P. von Grebe, P. J. Sanz Miguel, F. Pichierri, A. Springer, C. A. Schalley and B. Lippert, *Dalton Trans.*, 2011, **40**, 5159–5161.
24 K. F. Konidaris, C. N. Morrison, J. G. Servetas, M. Haukka, Y. Lan, A. K. Powell, J. C. Plakatouras and G. E. Kostakis, *CrystEngComm*, 2012, **14**, 1842.
25 G. Mahmoudi, A. Castiñeiras, P. Garczarek, A. Bauzá, A. L. Rheingold, V. Kinzhybalo and A. Frontera, *CrystEngComm*, 2016, **18**, 1009–1023.
26 S. Bhattacharya, S. Roy, K. Harms, A. Bauza, A. Frontera and S. Chattopadhyay, *Inorganica Chim. Acta*, 2016, **442**, 16–23.
27 J. P. Blagojević and S. D. Zarić, *Chem. Commun.*, 2015, **51**, 12989–12991.
28 E. C. Lee, D. Kim, P. Jurečka, P. Tarakeshwar, P. Hobza and K. S. Kim, *J. Phys. Chem. A*, 2007, **111**, 3446–3457.
29 M. Rapacioli, F. Spiegelman, D. Talbi, T. Mineva, A. Goursot, T. Heine and G. Seifert, *J. Chem. Phys.*, 2009, **130**, 244304.
30 D. P. Malenov, D. B. Ninković, D. N. Sredojević and S. D. Zarić, *ChemPhysChem*, 2014, **15**, 2458–2461.
31 D. P. Malenov, D. Ž. Veljković, M. B. Hall, E. N. Brothers and S. D. Zarić, *Phys. Chem. Chem. Phys.*, 2019, **21**, 1198–1206.
32 D. B. Ninković, J. M. Andrić and S. D. Zarić, *ChemPhysChem*, 2013, **14**, 237–243.
33 D. P. Malenov and S. D. Zarić, *Phys. Chem. Chem. Phys.*, 2018, **20**, 14053–14060.
34 B. Jeziorski, R. Moszynski and K. Szalewicz, *Chem. Rev.*, 1994, **94**, 1887–1930.
35 E. G. Hohenstein and C. D. Sherrill, *J. Phys. Chem. A*, 2009, **113**, 878–886.
36 E. M. Cabaleiro-Lago and J. Rodríguez-Otero, *ChemistrySelect*, 2017, **2**, 5157–5166.
37 R. M. Parrish, L. A. Burns, D. G. A. Smith, A. C. Simmonett, A. E. DePrince, E. G. Hohenstein, U. Bozkaya, A. Y. Sokolov, R. Di Remigio, R. M. Richard, J. F. Gonthier, A. M. James, H. R. McAlexander, A. Kumar, M. Saitow, X. Wang, B. P. Pritchard, P. Verma, H. F. Schaefer, K. Patkowski, R. A. King, E. F. Valeev, F. A. Evangelista, J. M. Turney, T. D. Crawford and C. D. Sherrill, *J. Chem. Theory Comput.*, 2017, **13**, 3185–3197.
38 E. G. Hohenstein and C. D. Sherrill, *J. Chem. Phys.*, 2010, **132**, 184111.
39 E. G. Hohenstein, R. M. Parrish, C. D. Sherrill, J. M. Turney and H. F. Schaefer, *J. Chem. Phys.*, 2011, **135**, 174107.
40 J. F. Gonthier and C. D. Sherrill, *J. Chem. Phys.*, 2016, **145**, 134106.
41 C. D. Sherrill, *Acc. Chem. Res.*, 2013, **46**, 1020–1028.
42 H. Li, E. N. Brothers and M. B. Hall, *Inorg. Chem.*, 2014, **53**, 9679–9691.

View Article Online
DOI: 10.1039/C9DT00182D

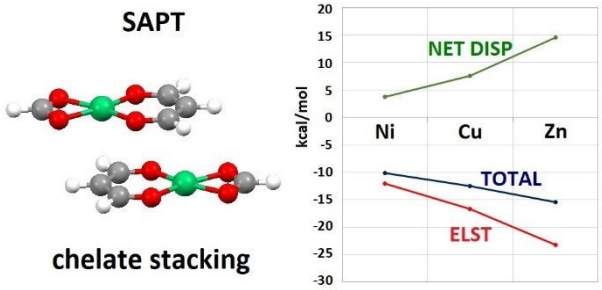

Stacking interactions of metal-chelate rings are strong due to very strong electrostatic energy component.